Title: A functional genomic screen identifies the deubiquitinase USP11 as a novel transcriptional regulator of ERα in breast cancer

Running title: The role of USP11 in ERα function in breast cancer

Lisa Dwane[1], Aisling E. O'Connor[2], Sudipto Das[1], Bruce Moran[2], Laoighse Mulrane[2], Adan Pinto-Fernandez[3], Elspeth Ward[1], Anna M. Blümel[1], Brenton L. Cavanagh[4], Brian Mooney[1], Annette M. Dirac[5], Karin Jirström[6], Benedikt M. Kessler[3], Tríona Ní Chonghaile[7], René Bernards[5*], William M. Gallagher[2*] and Darran P. O'Connor[1*]

[1]School of Pharmacy and Biomolecular Sciences, Royal College of Surgeons Ireland, 123 St. Stephen's Green, Dublin 2, Ireland.
[2]Cancer Biology and Therapeutics Laboratory, UCD School of Biomolecular and Biomedical Science, UCD Conway Institute, University College Dublin, Dublin 4, Ireland.
[3]Target Discovery Institute, Nuffield Department of Medicine, University of Oxford, Headington, UK.
[4]Cellular and Molecular Imaging Core, Royal College of Surgeons in Ireland, 123 St. Stephen's Green, Dublin 2, Ireland
[5]Division of Molecular Carcinogenesis, Oncode Institute, Netherlands Cancer Institute, Amsterdam, the Netherlands.
[6]Division of Oncology and Pathology, Department of Clinical Sciences Lund, Lund University, Lund, Sweden.
[7]Department of Physiology and Medical Physics, Royal College of Surgeons Ireland, 123 St. Stephen's Green, Dublin 2, Ireland.

*Shared Senior Authorship

Correspondence should be directed to Prof. Darran O'Connor, Associate Professor of Molecular Oncology, School of Pharmacy and Biomolecular Sciences, Royal College of Surgeons in Ireland, Dublin 2, Ireland. T: +353 1 402 2596; E: darranoconnor@rcsi.com

The authors declare no potential conflicts of interest in relation to the work described.

Abstract

Approximately 70% of breast cancers express estrogen receptor α (ERα) and depend on this key transcriptional regulator for proliferation and differentiation. While patients with this disease can be treated with targeted anti-endocrine agents, drug resistance remains a significant issue, with almost half of patients ultimately relapsing. Elucidating the mechanisms that control ERα function may further our understanding of breast carcinogenesis and reveal new therapeutic opportunities. Here we investigated the role of deubiquitinases (DUB) in regulating ERα in breast cancer. An RNAi loss-of-function screen in breast cancer cells targeting all DUB identified USP11 as a regulator of ERα transcriptional activity, which was further validated by assessment of direct transcriptional targets of ERα. USP11 expression was induced by estradiol (E2), an effect that was blocked by tamoxifen and not observed in ERα-negative cells. Mass spectrometry revealed a significant change to the proteome and ubiquitinome in USP11 knockdown cells in the presence of E2. RNA sequencing in LCC1 USP11 knockdown cells revealed significant suppression of cell cycle-associated and ERα target genes, phenotypes that were not observed in LCC9 USP11 knockdown, anti-endocrine resistant cells. In a breast cancer patient cohort coupled with in silico analysis of publicly available cohorts, high expression of USP11 was significantly associated with poor survival in ERα-positive patients. Overall, this study highlights a novel role for USP11 in the regulation of ERα activity, where USP11 may represent a prognostic marker in ERα-positive breast cancer.

Significance

A newly identified role for USP11 in ERα transcriptional activity represents a novel mechanism of ERα regulation and a pathway to be exploited for the management of ER-positive breast cancer.

Introduction

Approximately 70% of breast cancers express estrogen receptor α (ERα) and depend on this key transcriptional regulator for growth and differentiation. Patients with ERα-positive (ERα+) breast cancer are treated with targeted, anti-endocrine therapies. Despite advancements in targeted treatment options, drug resistance remains a clinically significant problem, with almost half of patients eventually relapsing on endocrine intervention therapies (1). As such, the discovery of novel mechanisms controlling ERα function in breast cancer represent major advances in our understanding of breast cancer progression and may offer new therapeutic opportunities. In this study, we investigated the role of deubiquitinases (DUBs), a class of enzymes that remove ubiquitin moieties from target proteins, in ERα function in breast cancer.

Ubiquitination, a post-translational modification (PTM) involving the addition of a ubiquitin (Ub) moiety to a target protein, is the primary mechanism of protein turnover in the cell. This is a complex, multistep biochemical pathway that ultimately leads to a mono- or polyubiquitinated target protein. Polyubiquitin chains are generated using any of the seven lysine residues on Ub itself, with different chain topologies resulting in different functional consequences. Polyubiquitin chains linked at lysine (K) residue 48 (K48) shuttle the tagged protein to the 26S proteasome for degradation (2). On the other hand, monoubiquitination and Ub chains of different topologies result in altered target protein functionality and drive pathways such as endocytosis (3) and DNA damage repair (4).

Like most other PTMs, ubiquitination is a reversible process. By hydrolysing the isopeptide bond between Ub and the target protein, DUBs remove ubiquitin molecules from ubiquitinated proteins, stabilising the target and preventing proteasomal degradation. Furthermore, DUBs also play a vital role in Ub recycling, generation of Ub precursors and protecting the proteasome from free Ub chains (5). The mammalian genome encodes for over 100 DUBs, which are classified into six different groups based on their sequence and structure similarity. Aside from the Jabb1/MPN domain-associated metalloproteases (JAMM) DUB family, all DUBs are cysteine proteases, and utilise a catalytic dyad or triad of amino acids to hydrolyse the isopeptide bond between Ub and the target protein. The largest and most diverse DUB family are the ubiquitin-specific proteases (USPs); it is predicted that the

human genome encodes over 50 of this class (6). The USP DUBs encode highly conserved Cys and His box motifs, which contain all catalytic triad residues.

DUBs are often differentially expressed or activated in tumours, and targeting them in the clinic has now become an area of therapeutic interest. Recently, the role of DUBs in nuclear receptor signalling in various cancers has been highlighted in the literature. For example, USP7 regulates the androgen receptor (AR) in prostate cancer by deubiquitinating AR in an androgen-dependent manner, associating with AR at androgen responsive elements and facilitating chromatin binding (7). Moreover, AR is also regulated by USP26 in a similar manner (8), highlighting an integral role for DUBs in AR signalling. ERα, on the other hand, is deubiquitinated by Otubain-1 (OTUB1) *in vitro*. OTUB1 negatively regulates transcription of the ERα gene itself and can stabilise the receptor in endometrial cancer cells (9). USP9x is also a key ERα interactor. USP9x attenuation was found to render breast cancer cells resistant to tamoxifen, leading to the generation of a gene signature used to define patient outcome following adjuvant tamoxifen treatment (10).

Given the accumulating evidence for nuclear receptor regulation by DUBs, we sought to identify the role of DUBs in ERα function by taking an unbiased, functional genomics approach. An RNA interference (RNAi) loss-of-function screen targeting all known or putative DUBs in the human genome was performed. Interestingly, silencing of the BRCA2-associated DUB USP11 (11) was found to suppress ERα transcriptional activity. USP11 is a protease with multiple cellular functions including the positive regulation of TGFβ signalling and stabilisation of inhibitor of apoptosis (IAP) proteins (12,13). Perhaps the most widely studied function of USP11, however, is its role in homologous recombination (14,15). Until now, the role of USP11 in ERα function remained unknown. This study provides strong evidence for the role of USP11 in ERα transcriptional function and identifies USP11 as a marker of poor prognosis in ERα-positive (ERα+) breast cancer. We believe that USP11 may be a viable therapeutic target in ERα+ breast cancer, offering treatment options for patients who do not respond to or relapse on currently available therapies.

Methods

Cell lines and culture

ZR-75-1, T47D, SUM44, MDA-MD-134VI and CAMA-1 cells were purchased from the American Tissue Culture Collection (www.atcc.org). MCF7, LCC1 and LCC9 cells were a kind gift from Prof. Robert Clarke (Georgetown University Medical School, Washington DC, USA). HEK293T wild type and USP11 knockout cell lines were a kind gift from Dr. Daniel Durocher (The Lunenfeld-Tanenbaum Research Institute, Mount Sinai Hospital, Toronto, Ontario, Canada). ZR-75-1, MCF7 and HEK293T cells were cultured in Dulbecco's Modified Eagle Medium (DMEM) (Sigma-Aldrich, St Louis, MO, USA) supplemented with 10% Foetal Bovine Serum (FBS) (v/v) (Gibco, Invitrogen, Carlsbad, CA, USA), 1% penicillin/streptomycin (v/v) (Gibco, Invitrogen) and 1% L-glutamine (Gibco, Invitogen). ZR-75-1 culture media was also supplemented with 1 nM estradiol (E2) (Sigma-Aldrich). T47D, SUM44, MDA-MB-134VI and CAMA-1 were cultured in RPMI-1640 (Sigma-Aldrich) supplemented with 10% Foetal Bovine Serum (FBS) (v/v) (Gibco, Invitrogen, Carlsbad, CA, USA), 1% penicillin/streptomycin (v/v) (Gibco, Invitrogen) and 1% L-glutamine (Gibco, Invitogen).

LCC1 and LCC9 cells were cultured in phenol red-free DMEM (Sigma-Aldrich) supplemented with 5% charcoal/dextran-treated Foetal Bovine Serum (FBS) (v/v) (Gibco, Invitrogen), 1% penicillin/streptomycin (v/v) (Sigma-Aldrich) and 1% L-glutamine (Gibco, Invitrogen). Experiments which required hormone depletion were also cultured in phenol red-free media.

Sub-culturing of all cells took place in a Class II laminar flow hood under sterile conditions. ZR-75-1 stable USP11 knockdown (KD) cell lines were generated following transduction of two independent lentiviral shRNAs and a non-targeting control (NTC) shRNA. To achieve transient USP11 knockdown, two independent ON-TARGETplus siRNAs (Dharmacon) targeted to USP11 (30 nM) were transfected into cells using lipofectamine 2000 (Invitrogen) (all sequences in Supplementary Table 1). An ON-TARGETplus SMARTpool control (30 nM; Invitrogen) was used a negative control. Knockdown was assessed 72-120 hours post-transfection, depending on the assay performed). To examine ERα function in HEK293T cells, cells were transfected with HA-ERα (addgene #49498) using lipofectamine 3000 (Invitrogen).

171
172
173 **RNAi screen**

174 ZR-75-1 cells were seeded in 24-well plates in antibiotic-free media, 24 hours
175 prior to transfection. The shRNA DUB library used, generated at the Netherlands
176 Cancer Institute (NKI), Amsterdam and previously described in the literature by
177 Brummelkamp and colleagues (16), contained four non-overlapping shRNAs
178 targeted to each DUB (108 DUBs, 432 shRNAs in total). shRNAs were transfected
179 with estrogen response element (ERE) luciferase and CMV renilla reporters
180 described previously (10), the latter representing an internal control. Cells were
181 transferred to hormone-depleted media for 48 hours before stimulation with 1 nM E2
182 for 24 hours. Cells were harvested and luciferase activity was measured using the
183 Dual Luciferase Reporter assay system (Promega, WI, USA) as per manufacturer's
184 instructions. Hairpins demonstrating no net effect served as internal controls. Results
185 were confirmed in biological triplicate in the presence and absence of E2.
186
187 **Western blotting**

188 Protein samples were diluted in an appropriate volume of 4X NuPAGE Lithium
189 Dodecyl Sulfate (LDS) buffer (Invitrogen), supplemented with 2.5% β-
190 Mercaptoethanol (Sigma-Aldrich). Samples were boiled at 100˚C for 5 minutes to
191 allow for protein denaturation before loading onto the gel. SDS-PAGE was
192 performed in 1X Tris Glycine running buffer (25 mM Tris, 250 mM glycine, 0.1%
193 SDS) using a Bio-Rad Mini Protean III gel system (Bio-Rad Laboratories, Hercules,
194 CA, USA). Gels were run for approximately 20 minutes at 90V through the stacking
195 gel, followed by approximately 60 minutes at 120V through the resolving gel.
196 Resolved proteins were transferred to a nitrocellulose membrane in 1X
197 transfer buffer (25 mM tris, 190 mM glycine, 20% methanol) using a Bio-Rad Mini-
198 Protean III electrophoretic transfer cell (Bio-Rad) at 300 mA for 90 minutes at 4˚C.
199 Following transfer, membranes were blocked with either 5% (w/v) non-fat dried milk
200 (Sigma-Aldrich) or 5% (w/v) BSA (Sigma-Aldrich), both prepared in 100 mL of 1X
201 TBS buffer containing 0.1% (v/v) Tween 20 (Sigma-Aldrich), and incubated with
202 gentle agitation for 1 hour at room temperature. Membranes were then incubated in
203 blocking buffer containing the primary antibody of choice overnight at 4˚C.

Following primary antibody incubation, membranes were washed with TBS-T and subsequently incubated for 1 hour at room temperature with horseradish peroxidise (HRP)-conjugated secondary antibody (anti-mouse/anti-rabbit, Dako, Glostrup, Denmark) contained in blocking buffer. Membranes were again washed in TBS-T and detection of HRP complexes was achieved by exposing the membranes to Enhanced Chemiluminescence (ECL) substrate (Pierce). Membranes were imaged using the Amersham Imager 600 (GE Healthcare Life Sciences, Marlborough, MA, USA).

Sub-cellular fractionation

ZR-75-1 cells were seeded and transferred to phenol red-free DMEM containing 5% charcoal/dextran-treated FBS. After 48 hours, cells were stimulated with either vehicle (EtOH) or 1 nM E2. Cellular fractions were generated using Qiagen's Cell Compartment kit, as per manufacturer's instructions. Extracts were analysed using Western blotting, with anti-GAPDH, anti-trimethyl histone H3 and anti-cytochrome-C antibodies used as cytosolic, nuclear and membrane markers, respectively.

Immunocytochemistry (ICC)

ZR-75-1 cells were seeded in to 8-well chamber slides in hormone-depleted media at a density of 100,000 cells per well. After 48 hours, cells were stimulated with 1 nM E2 for either 4 or 24 hours, or left in hormone-depleted conditions.

Media was aspirated, cells were washed in PBS and subsequently fixed in 100% methanol for 20 minutes. The cells were washed 2 x 5 minutes in PBS before blocking in 10% goat serum in 5% w/v BSA/PBS for 60 minutes. The cells were washed in PBS for 5 minutes before a 90 minute incubation in the primary antibody (USP11 1:250) diluted in 10% human serum in 5% w/v BSA/PBS. The cells were washed 2 x 5 minutes in PBS to remove excess primary antibody. The cells were then incubated in secondary antibody (Alex Fluor® 594, 1:200) diluted in 10% human serum in 5% w/v BSA/PBS, for 60 minutes, and the slide was covered in tin foil to protect from light. The cells were washed 2 x 5 minutes in PBS before mounting the cover slip on to the chamber slide. A small volume of Vectashield mounting medium containing DAPI (Vector Laboratories, CA, USA) was placed on

the slide and the coverslip was gently lowered on to the slide. The coverslip was sealed using clear nail polish.

Widefield fluorescent microscopy was carried out using a Nikon Eclipse 90i equipped with a DS-Ri1 camera and Plan Fluor 20x (N.A 0.5) objective paired with DAPI and TRITC filtersets. NIS-Elements BR 3.10 was used to capture images with fixed acquisition settings.

A Carl Zeiss LSM 710 equipped with a W Plan-Apochromat 20x objective (N.A 1.0) was used to capture confocal images with fixed acquisition settings. Samples were simultaneously excited with 405 and 594 nm lasers and the resulting emissions captured using spectral detectors over the range of 409 – 495 and 598 – 726nm respectively. 4x averaging and a spacing of 0.806 µm was used when capturing z stacks in the Zen 2008 software.

FIJI (17) was used for the preparation of both widefield and confocal images. All z stacks are presented as maximum image projections.

qRT-PCR

RNA was extracted in Tri-Reagent (Sigma-Aldrich) and quantified using a NanoDrop UV-Vis spectrophotometer (Thermo Fisher Scientific) according to manufacturer's instructions. RNA samples were diluted in nuclease-free water to yield the same concentration per sample and were treated with DNase I (Invitrogen) to remove genomic DNA from the samples. cDNA was synthesised using the high capacity cDNA reverse transcription kit (Invitrogen) as per manufacturer's instructions. Samples were incubated in the Bio-Rad T100 Thermal Cycler (BioRad) at 25˚C for 10 minutes, followed by 37˚C for 60 and 85˚C for 5 minutes.

cDNA was diluted in 2X SYBR green (Promega), forward and reverse primers (Eurofins MWG, Kraainem, Belgium) and dH_2O in a 96-well plate. qRT-PCR was performed using the Applied Biosystems 7500 real-time PCR system set to the following temperature cycles: 2 minutes at 50˚C, 10 minutes at 95˚C, followed by 40 cycles oscillating between 15 seconds at 95˚C and 1 minute at 60˚C. A melting curve was generated after each run in order to ensure primer specificity: 15 seconds at 95˚C, 15 seconds at 60˚C and 15 seconds at 95˚C. Primer sequences can be found in Supplementary Table 1.

RNA sequencing

Both LCC1 and LCC9 cell lines were transfected with two independent siRNAs targeted to USP11 and a siRNA non-targeting control (NTC) using lipofectamine 2000, as described above. Cells were incubated for 72 hours before extraction of RNA. Samples were prepared in biological triplicate.

cDNA libraries were prepared from RNA samples using Illumina's neoprep library card, as per manufacturer's instructions. Samples were prepared for sequencing on the NextSeq 500 (Illumina) as per manufacturer's instructions. Two x 75 bp paired-end reading was performed.

For bioinformatic analysis, Fastq files were downloaded from Illumina BaseSpace using the BaseSpace download tool (https://github.com/ReddyLab/BaseSpaceFastqDownload).
The quality of Fastq files was determined using FastQC: (https://www.bioinformatics.babraham.ac.uk/projects/fastqc/).
Reads were trimmed to remove poor quality base calls (Phred score < 20) and sequencing adaptors, using BBDuk tool in the BBMap package (https://jgi.doe.gov/data-and-tools/bbtools/bb-tools-user-guide/bbmap-guide/).

Sequencing reads were aligned to the human hg19/GRCh37 genome reference using the STAR alignment algorithm, version 2.5.2a (18). This produced a BAM file which was sorted by coordinate. Duplicate reads were marked in the BAM using Picard-Tools 'MarkDuplicates' call (https://broadinstitute.github.io/picard/). Read counts were produced by the featureCounts tool from the SubRead package (19). These counts were combined for all samples and used as input for differential gene expression analysis.

Differential Expression

Differential expression (DE) analysis of genes was carried out using the DESeq2 package (20) in the R statistical environment (R Development Core Team, 2012). The data.frame of counts had all genes with a sum of zero across all samples removed. A 'conditions' data.frame was created based on the sample names, their group (i.e. LCC1_control, LCC1_si7, LCC1_si8, LCC9_control, LCC9_si7 or LCC9_si8) and their biological replicate number. The counts and conditions data.frames were loaded into a DESeq2DataSet class object using the DESeqDataSetFromMatrix() call, with the design variable set as '~ group'. the DESeq() call produced two sets of results, based on LCC1 or LCC9 cells, comparing

the two individual siRNA knockdowns to the control for each cell line. Four text files resulted, containing each gene expressed, the log2FoldChange value and the FDR adjusted p-value. Principal component analysis plots were produced for the full dataset to determine the quality of the count data and similarity of samples from the 6 conditions. These followed the standard protocol from the DESeq2 guide (https://bioconductor.org/packages/release/bioc/vignettes/DESeq2/inst/doc/DESeq2.html). Fragments-per-kilobase per million reads (FPKMs) were produced using the edgeR package (21) rpkm() call.

RNA-seq was validated using qRT-PCR as described above, using the same sequenced RNA samples.

Enrichment analysis

DE genes were subject to gene ontology (GO) enrichment analysis in order to detect altered cellular pathways following USP11 knockdown. The Database for Annotation, Visualisation and Integrated Discovery (DAVID) (http://david.abcc.ncifcrf.gov/) was used for GO and Kyoto Encyclopaedia of Genes and Genomes (KEGG) pathway enrichment (22). Significantly DE genes, grouped according to whether they were up- or downregulated with USP11 knockdown, were input into DAVID for enrichment analysis. An FDR (False Discovery Rate) <5% was considered statistically significant.

Gene Set Enrichment Analysis (GSEA) is an improved method of analysis to define the biological functions of gene sets (23). The method uses weighted genes according to their correlation with phenotype rather than equal weights for each gene. GSEA 3.0 and gene sets were downloaded from the Molecular Signatures Database (MsigDBv3.1). Phenotypes were assigned to both knockdown and control samples and enrichment analysis was carried out against a defined gene set. The GSEA procedure was performed as follows; an enrichment score (ES) was calculated ranking genes according to their differential expression and a nominal P value was obtained as an estimate of the significance level of the enrichment score. Subsequently, the enrichment score was normalised (NES) and FDR was calculated to adjust for multiple hypothesis testing.

Immunoaffinity purification (IAP) and mass spectrometry

ZR-75-1 USP11 knockdown and NTC cells were processed as described previously (24). In brief, cells were lysed in urea lysis buffer, and proteins were digested by sonication. DTT and iodoacetamide were used to reduce and alkylate the samples, respectively. Samples were further digested overnight at room temperature using trypsin, and protein digestion was confirmed using SDS-PAGE. To remove fatty acids, acidification of samples was performed using trifluoroacetic acid (TFA). Samples were treated with a final concentration of 1% TFA, and centrifuged at 1,780 *x g* for 15 minutes at RT to isolate fatty acid precipitates. Proteins were purified using the Sep-Pak® C18 system, as per manufacturer's instructions.

The lyophilized peptide was centrifuged at 2000 *x g* at RT for 5 minutes. All samples were resuspended in 1.4 mL IAP buffer and transferred to a 1.7 mL reaction tube. A neutral pH was confirmed and samples were centrifuged at 10,000 *x g* for 15 minutes at 4°C. UbiScan® beads were washed four times with PBS, centrifuged at 2000 *x g* for 30 seconds between each wash. The beads were resuspended in 40 µL PBS following the final wash. The supernatant from the peptide solution was added to the beads and all samples were incubated at 4°C for 2 hours with constant agitation.

The flow-through was transferred to a new reaction tube and stored. The beads were washed with 1X IAP buffer two times, centrifuged at 2000 *x g* for 30 seconds at 4°C between each wash. The beads were then washed with water three times, centrifuged at 2000 *x g* for 30 seconds at 4°C between each wash. Fifty-five µL of 0.15 % TFA was added to each tube of beads and mixed gently. Samples were left to incubate at room temperature for 10 minutes, mixing gently every two minutes. The samples were centrifuged at 2000 *x g* for 30 seconds and the supernatant was collected in a new tube. This elution step was repeated. Peptides were concentrated and purified using the StageTip protocol, as per manufacturer's instructions, and prepared for liquid chromatography mass spectrometry (LC-MS).

Mass Spectrometry and Proteomics Data Analysis

Samples prepared as described above were analysed by liquid chromatography tandem mass spectrometry (LC-MS/MS) as described previously (24). To convert MS spectra generated from the Q Exactive Hybrid Quadrupole-Orbitrap Mass Spectrometer (Thermo Scientific) to protein identifications, the

MaxQuant (25) computational platform (version 1.5.2) was used. Label-free quantification (LFQ) values were extracted from the protein groups (proteome) and peptides (ubiquitome) previously generated by MaxQuant, and uploaded to the Perseus computational platform (version 1.6.1.1) (26). Statistical analysis of the identified and quantified proteins was handled using the Perseus software package. A histogram showing counts versus label-free quantification (LFQ) intensity was generated for each sample to highlight the distribution of counts, and the imputation performed previously. Principle component analysis (PCA) was performed on samples in order to demonstrate how each sample grouped respective to all other samples. To highlight differentially expressed proteins between any two groups, a volcano plot was generated using a two-sided t-test (unpaired). The false discovery rate (permutation FDR for multiple testing) for all volcano plots was set to 5% (0.05), and the s0 LFQ difference value was kept at the default 0.1.

Immunohistochemistry

Immunohistochemistry was performed using the Ultravision LP Large Volume Detection System HPR polymer (Labvision) and DAB Plus Substrate System (Labvision). Slides were incubated for 10 minutes in 3% H_2O_2 to block endogenous peroxidases and then washed with phosphate-buffered saline 0.1% v/v Tween (PBS-T). Protein block was applied for 5 minutes before incubation with anti-USP11 primary antibody (Bethyl Laboratories, Texas, USA) for 60 minutes. Slides were then washed and incubated with secondary antibody solution (primary antibody enhancer) for 10 minutes and washed again with PBS-T. Finally, slides were incubated in HRP-polymer for 15 minutes, washed with PBS-T and incubated in 3, 3'-diaminobenzidinetrahydrochloride (DAB) for 10 minutes. Slides were then counterstained by a 3 minute exposure to haematoxylin and subsequent agitation in tepid dH_2O. Slides were dehydrated in ascending concentrations of ethanol in Coplin jars as follows: 3 minutes in 80% v/v ethanol, 3 minutes in 95% v/v ethanol, 2 x 3 minutes in 100% v/v ethanol and 2 x 3 minutes in xylene. Slides were then mounted in Permount mounting medium (Thermo Fisher Scientific) using an automated cover-slipper (Leica Microsystems). Slides were scanned using a ScanScope XT Digital Slide Scanner (Aperio Technologies, CA, USA) and analysed using ImageScope software (Aperio Technologies).

406 **Patient cohort**

407 The TMA cohort used in this study, described previously in the literature by
408 DeNardo et al. (27), was generated from a consecutive cohort of 144 patients
409 diagnosed with invasive breast cancer in Malmo University Hospital, Sweden, in
410 2001 and 2002. These patients did not receive any neoadjuvant treatment prior to
411 surgery. One hundred and three (72%) of the patients had ER-positive tumours, and
412 complete data on anti-endocrine therapy were available for 95 patients; 77 of whom
413 received tamoxifen, 3 an aromatase inhibitor and 25 a combination of both. Thirty
414 patients received adjuvant chemotherapy and 83 received radiotherapy. At the time
415 of the last follow-up, 41 patients had passed away, 22 of whom as a direct result of
416 breast cancer. USP11 expression and its association with overall, recurrence-free
417 and breast cancer-specific survival were the primary endpoints of focus.

418

419 **Statistical analysis**

420 *In silico* analysis of publically available breast cancer datasets was carried out
421 using Gene Expression Based Outcome (GOBO) (28), where differences were
422 outlined in overall survival (OS), distant metastasis-free survival (DMFS) and
423 recurrence-free survival (RFS) according to USP11 expression. A p-value <0.05 was
424 considered statistically significant.

425 For TMA analysis, biopsy cores were manually scored (0-3) based on the
426 degree of DAB positive staining. Kaplan-Meier and Cox regression analysis was then
427 used to determine differences in OS, RFS and breast cancer-specific survival
428 (BCSS) according to USP11 expression. Pearson's chi-squared test was used to
429 evaluate associations between USP11 expression and clinicopathological
430 characteristics. SPSS version 20.0 (SPSS Inc, Chicago, IL, USA) was used to carry
431 out statistical analysis of TMA-derived data, and a p-value <0.05 was considered
432 statistically significant.

433 GraphPad Prism 5 was used to carry out statistical analysis on all *in vitro*
434 work. Student's t-test/one-way ANOVA statistical tests were used, with a p-value
435 <0.05 considered statistically significant.

436

437

438

439

Results

Loss of USP11 negatively regulates ERα transcriptional activity

In order to determine the role of DUBs in ERα transcriptional function in breast cancer cells, an unbiased RNAi loss-of-function screen was performed, targeting all 108 known or putative DUBs in the human genome. The library contained four non-overlapping shRNAs targeted to each DUB, 432 in total. Each pool was co-transfected into ZR-75-1 ERα+ breast cancer cells along with estrogen response element-luciferase (ERE-luc) and CMV-renilla reporters, in order to detect transcriptional activity of ERα following estradiol (E2) stimulation with suppression of each DUB (Figure 1A). DUB knockdown led to repressed, enhanced or unchanged activity at the ERE-luc reporter (Figure 1B). A selection of DUBs were chosen for triplicate validation of the RNAi screen in both the presence and absence of E2. The DUBs selected included 5 that repressed activity, 5 that enhanced activity, and 5 that unchanged activity (serving as baseline controls) at the ERE-luc reporter from the RNAi screen. This validation experiment supported the results obtained from the RNAi screen (Figure 1C) with all selected DUBs displaying the same phenotype as previously observed. Interestingly, the two DUBs whose knockdown suppressed ERα transcriptional activity to the greatest extent were OTUB-1 and USP11. As mentioned, a previous study has demonstrated that ERα is deubiquitinated by OTUB1, which regulates its transcriptional activity in endometrial cancer cells (9). USP11 has been previously associated with the BRCA proteins (11) and is a key enzyme in the DNA-damage response (14,15); however, its role in ERα function has not been reported previously. We hypothesised from the loss-of-function DUB screen that USP11 is a novel regulator of ERα transcription and may represent a target of interest in ERα+ breast cancer.

USP11 silencing abrogates ERα target gene expression

In order to validate the results obtained from the RNAi screen, HEK293T USP11 knockout cells were used to examine the impact of USP11 function on ERα activity. Cells were transfected with an ERα expression vector (HA-ERα) (Figure 1D) and ERE-luc and CMV-renilla reporters. ERα activity was significantly suppressed in USP11 knockout cells following stimulation with E2 (Figure 1E), further supporting a role for USP11 in regulating ERα transcriptional activity, as first demonstrated in the RNAi screen. The induction of two ERα-target genes, progesterone receptor *(PgR)* and tre-foil factor 1 (*TFF1),* following E2 stimulation was also suppressed in USP11 knockout cells (Figure 1F & G). To validate this in a breast cancer model, USP11 was knocked down in ZR-75-1 breast cancer cells using two individual siRNAs targeted to USP11. Knockdown was confirmed 72 hours post-transfection using qRT-PCR (Figure 1H). The mRNA expression of ERα target genes were subsequently examined and the expression of *PgR* and *TFF1* were notably suppressed following USP11 silencing (Figure 1I & J).

Estradiol (E2) increases the expression of USP11

Next, the expression of USP11 was examined in a panel of ERα+ breast cancer cell lines (ZR-75-1, T47D, MCF7, LCC1, LCC9, CAMA-1, MDA-MB-134VI and SUM44). Basal expression of USP11 varied from low to high across all cell lines, however, expression levels correlated with ERα expression (Figure 2A). This was confirmed by densitometric and statistical analysis (Pearson r: 0.76; p-value: 0.027) (Figure 2B). Subsequently, we investigated whether USP11 expression was regulated by E2 and if any changes were affected by the presence of 4-hydoxytamoxifen (4-HT). ZR-75-1 and MCF7 cells were stimulated with either 1 nM E2 alone or 1 nM E2 combined with 1 μM 4-HT over a time course (4, 24 and 48 hours). USP11 protein expression was increased following E2 exposure in a time dependant manner in both cell lines, as determined by Western blotting. Remarkably, this change in expression was blocked in the presence of 4-HT (Figure 2C). As expected, ERα protein expression was initially repressed following E2 exposure (4 hr) and re-expressed later (24 and 48 hrs); an effect that was

antagonised by 4-HT. ERα protein expression therefore serves as a valuable control to E2/4-HT treatment. Further to this, MDA-MB-231, ERα-negative breast cancer cells were also examined for change in USP11 expression following E2/4-HT exposure. Neither compounds had an effect on USP11 expression (Figure 2C).

To assess localisation of USP11 following E2 treatment, protein sub-cellular fractions were generated, allowing for analysis of the nuclear, cytoplasmic, and membrane proteins within the cell. USP11 expression was upregulated in the nucleus of ZR-75-1 cells following E2 stimulation in a time-dependent manner (Figure 2D). This result was supported using immunocytochemistry and confocal microscopy, where expression of USP11 was found to be upregulated in the nucleus following E2 treatment (Figure 2E).

This evidence strongly suggests that USP11 is regulated by E2, via ERα, perhaps in a positive feedback loop to enhance ERα transcriptional activity. The exact mechanism, and whether this occurs via a direct or indirect effect of ERα, warrants further investigation.

USP11 suppression significantly alters the proteome and ubiquitinome in breast cancer cells in the presence of E2

The data presented above supports a key role for USP11 in ERα transcriptional function, and demonstrates that suppression of USP11 can abrogate the action of the receptor. To further explore this role, we sought to examine how USP11 modulation effects the proteome and ubiquitinome of ERα+ cells, and how these modulations are affected in the presence and absence of E2. To do so, we used mass spectrometry to analyse the proteome and ubiquitinome of USP11 knockdown (shUSP11_1, shUSP11_4) and control (NTC) ZR-75-1 cells, in both the presence and absence of E2 (Figure 3A). Hierarchical clustering of proteomic data demonstrated a unique proteomic pattern in the presence and absence of estrogen (Figure 3B). Next, both knockdown cell lines were each compared to NTC cells in order to examine individual protein changes among samples. A number of proteins are significantly upregulated in knockdown and control samples in the presence of E2 (Figure 3C & D). Strikingly, in the absence of E2, modulation of USP11 with

either hairpin had no significant effect on the proteome of ZR-75-1 cells (Figure 3E & F). This suggests that the role of USP11 in ZR-75-1 cells is highly dependent on E2.

We next examined differentially expressed proteins common to both knockdown samples. Proteins depleted in USP11 knockdown cells include macrophage migration inhibitory factor (MIF), a protein involved in the inflammatory pathway and cancer pathogenesis (29) and fatty acid binding protein 5 (FABP5), which has been implicated in several cancer types, including breast (30).

To analyse the USP11 ubiquitinome, we applied UbiScan, a technique that uses a ubiquitin remnant motif (K-ε-GG) antibody-bead conjugate to isolate ubiquitinated peptides (24,31). Digestion of proteins with trypsin during mass spectrometry sample preparation cleaves ubiquitin at the C-terminus, leaving a Gly-Gly residue (K-ε-GG) that is still attached to a lysine on the target protein, thus providing evidence of a ubiquitinated protein.

The USP11 ubiquitinome was analysed using a stable knockdown cell line (shUSP11_1) and control cells (NTC). Hierarchical clustering highlighted unique changes in ubiquitinated proteins in USP11 knockdown cells, predominantly in the presence of E2 (Figure 3G). This was supported with further analysis of individual ubiquitinated proteins where volcano plots highlighted a number of significant changes in ubiquitinated proteins in the presence of E2 following USP11 modulation (Figure 3H). Again, very few significant changes occurred in the absence of E2 (Figure 3I) further supporting the observation that USP11 function in ERα+ cells is highly regulated by E2. Interestingly, ubiquitination of γH2AX, a known substrate of USP11 (32) was increased following USP11 suppression, supporting the reliability of these results.

Proteins ubiquitinated following USP11 silencing may represent novel substrates and, in the presence of E2, may contribute to the role of USP11 in ERα transcriptional activity (Figure 3H, red dots). In order to decipher a link between USP11 and the receptor, the proteins significantly upregulated in USP11 knockdown cells when compared to control cells (USP11 ubiquitinome) were uploaded to STRING (version 10.5) to detect known and putative protein-protein interactions with ERα. The STRING search revealed several known, putative, direct and indirect ERα interactors (Supplementary Figure 1).

USP11 is upregulated in LCC1 cells and regulates ERα function

Our data above demonstrates that USP11 is a key regulator of ERα transcriptional activity and that its effects are highly dependent on estradiol and ERα itself. To further explore this, we chose to examine the effects of USP11 modulation in the LCC isogenic ERα+ cell line series (33,34). LCC1 cells remain responsive to anti-endocrine agents, suggesting that ERα still drives cellular growth, while LCC9 cells are anti-endocrine cross-resistant (fulvestrant and tamoxifen) and therefore no longer depend on ERα or estradiol for growth and survival. USP11 is significantly upregulated in both cell lines when compared to their parental MCF-7 cells, at both the protein and mRNA level (Figure 4A & B).

In order to investigate the role of USP11 on ERα transcriptional activity in each cell line, we examined the mRNA expression of the ERα+ target genes *PgR, PKIB* and *GREB1*. USP11 was knocked down using two independent siRNAs and knockdown was confirmed 72 hours post-transfection. USP11 silencing significantly decreased the mRNA expression of ERα target genes in LCC1 cells (Figure 4C). With the exception of moderately suppressed *PKIB* expression with one siRNA, no significant changes in expression occurred in LCC9 USP11 knockdown cells (Figure 4D).

To further elucidate the role of USP11 on ERα transcriptional activity in the LCC cell line model, RNA sequencing (RNA-seq) was performed on LCC1 and LCC9 USP11 knockdown cells (LCC1 siUSP11_1, siUSP11_2, siControl; LCC9 siUSP11_1, siUSP11_2, siControl; biological triplicate). First, principle component analysis (PCA) was carried out and values were plotted in order to visualise any variance between groups and replicates. Principle components were corrected for batch effect (Supplementary Figure 2A & B). Next, $\log_2$fold-change values of siControl samples were compared to each individual siUSP11 sample in order to determine genes which were differentially expressed (DE) following USP11 silencing. Both siRNA lists were compared and the common DE genes were subjected to further analysis, in order to minimise any off-target DE genes. In LCC1 cells, 278 DE genes were common to both siRNAs; in LCC9 cells, only 29 DE genes were common to both siRNAs (Figure 4E). DE genes in both cell lines were also compared. Only 9 genes were common to both cell lines (Figure 4F), demonstrating

a differential role for USP11 in cells that depend on ERα for growth and survival and those that depend on other mechanisms.

We examined genes that were both up- and down-regulated with knockdown in both cell lines (Figure 4G). In LCC1 cells, 188 genes were down-regulated (blue) and 90 were up (red) with USP11 suppression. In LCC9 cells, only 3 genes were down-regulated (blue) and 26 genes were up (red) with USP11 suppression. To further understand the effect of USP11 silencing on cellular function, these DE genes were subject to gene ontology (GO) analysis, a method which allows for the query of genes based on their shared biology (35). This allowed for the identification of key cellular pathways which are altered with USP11 silencing in LCC1 and LCC9 cells. Up- and down-regulated genes in each cell line were grouped for GO pathway analysis, completed using the Gene Set Enrichment Analysis (GSEA) 3.0 (23) bioinformatic tool. ENSEMBL gene IDs were uploaded and all GO biological concepts were analysed, including biological processes (BP), molecular function (MF) and cellular component (CC). Interestingly, knockdown of USP11 in LCC1 cells resulted in a significant decrease in cell cycle- and division-associated genes, consistent with the fact that LCC1 cells are still ERα-driven. Key cellular processes such as mitosis, chromosome segregation and organelle fission were all significantly downregulated with USP11 knockdown (Figure 4H). This phenotype was unique to LCC1 cells, suggesting that USP11 has a major role in controlling the cell cycle in cells dependent on ERα for growth (Figure 4I).

Conversely, knockdown of USP11 resulted in a significant increase in inflammatory-associated genes in both cell lines, identifying a common attribute of USP11 silencing in both LCC1 and LCC9 cells (Supplementary Figure 2C & D). In LCC1 USP11 knockdown cells, upregulated genes were associated with an innate immune response and interferon (INF) signalling, while the genes upregulated in LCC9 USP11 knockdown cells were primarily associated with viral response pathways. This is perhaps due to the role of USP11 in NFκB regulation (36).

A number of well-known ERα target genes were found to be significantly altered in LCC1 USP11 knockdown cells. For example, *TOP2A*, *BLM* and *BRCA1* were significantly downregulated according to RNA-seq data and confirmed by qRT-PCR analysis (Figure 4J). *TRIM22*, a target of p53 and a tumour suppressor gene (37), was upregulated in both LCC1 and LCC9 USP11 knockdown cells (Figure 4J).

LCC1 USP11 knockdown downregulated genes were then compared against GSEA curated genes sets, an online collection of datasets obtained from various sources such as the scientific literature and online pathway databases. Remarkably, one of the most significant overlapping genes sets was that published by Dutertre and colleagues (38), which is composed of 324 genes upregulated in MCF-7 cells treated with E2 for 24 hours. Of the 188 downregulated genes in the LCC1 USP11 knockdown list, 95 overlapped with the Dutertre dataset (p-value: 8.69 e-162; FDR q-value: 2.06 e-158; Figure 4K), suggesting that these are ERα target genes downregulated by USP11 silencing. We further examined ERα-positive, breast cancer patients in The Cancer Genome Atlas (TCGA) dataset and found that one-third (n= 102) of genes in the Dutertre dataset significantly correlated with USP11 in these patients. Of the 95 genes associated with the Dutertre gene set in LCC1 USP11 knockdown samples described above, 26 positively correlated with USP11 in TCGA samples, suggesting that expression of a subset of ERα target genes is significantly correlated with USP11 expression in breast cancer patients. (Supplementary Figure 3). These findings further support the pivotal role USP11 plays in controlling ERα transcriptional activity.

USP11 is a marker of poor prognosis in ERα+ breast cancer

Finally, the prognostic relevance of USP11 in ERα+ breast cancer was assessed in order to determine the validity of this protein as a marker in the clinic. Initially, an *in silico* analysis was performed using Gene Expression Based Outcome Online (GOBO) (http://co.bmc.lu.se/gobo/gsa.pl) (28). The online database, developed at Lund University, Sweden, consists of 1881 cases pooled from 11 public microarray datasets analysed using Affymetrix U133A. For survival analysis, two groups were selected; those with high expression of USP11 (red) and those with low expression (grey). Full censoring (years) was applied and overall survival (OS) was selected as the end point. High expression of USP11 was significantly associated with poor OS in ERα+ patients (p= 0.032; Figure 5A), while no significant association between USP11 expression and survival was made in ERα- patients (p= 0.51; Figure 5B). Multivariate analysis of the same datasets indicated that high USP11 expression was associated with tumour size, grade, and patients diagnosed over 50

years of age in the ERα+ cohort only (Figure 5C). These associations were not made in ERα-negative breast cancer patients (Figure 5D), suggesting that USP11 may be a useful prognostic marker in the ERα+ setting.

To support these findings, immunohistochemical staining of a TMA, described previously in the literature (27,39), with tumours samples from 144 cases of invasive breast cancer, diagnosed in Malmö University hospital between 2001 and 2002. The TMA consisted of 103 patients with ERα+ tumours for final analysis. Manual scoring was carried out by two independent researchers using the displayed images as guidance (Figure 5E). USP11 expression was grouped in to low (score 0 and 1) and high (score 2 and 3) expression and outcome based on each group was determined following statistical analysis of patient data. Kaplan-Meier analysis revealed a significant association between high USP11 expression and poor OS (p= 0.003; Figure 5F) and breast cancer-specific survival (BCSS) (p= 0.041; Figure 5G). A similar trend was observed between high USP11 expression and poor recurrence free survival (RFS) (p= 0.066; Figure 5, H). Cross tabulation analysis was also carried out in order to correlate USP11 staining with clinicopathological features such as tumour grade, histopathological subtype and hormone receptor status. High USP11 expression was significantly associated with positive lymph node status (p= 0.009), but not with any other clinicopathological features in this cohort.

Discussion

While our understanding and management of breast cancer is now better than ever, over 600,000 women worldwide succumb to this disease every year (40). Targeted, anti-endocrine therapies have been widely effective in treating patients with estrogen receptor alpha (ERα)-positive breast cancer, however, drug resistance and relapse remains a significant issue in the clinic. Given that the tumorigenic properties of ERα primarily lie in its function as a growth-controlling transcription factor, we sought to identify novel modulators of ERα transcriptional activity. Further understanding of the mechanisms that control ERα function are critical in order to design effective new targeted therapies, and while our knowledge of ERα function in breast cancer has vastly improved in recent years, translating this knowledge in to the clinical setting has proved challenging thus far.

The post-translational modifications of the receptor represent one such area of interest, with previous studies highlighting prominent roles for these modifications in determining receptor function in oncogenic pathways (10,41). Here, we focus on DUBs, the enzymes that reverse ubiquitination of proteins, and their role in ERα transcriptional activity. The oncogenic and tumour suppressive roles of these enzymes has come to light in recent years, and interest is growing in their therapeutic targeting as a result (42). We highlight for the first time, evidence for the role of the BRCA-associated (11,15) DUB USP11 in controlling ERα transcriptional activity. This represents a novel mechanism of ERα regulation in breast cancer and a pathway that could be exploited for the management of ERα-positive breast cancer.

In this study, functional genomic screening, examining the effect of DUB knockdown on ERα transcriptional activity in an unbiased fashion, identified a role for USP11 in ERα transcriptional regulation in breast cancer cells (Figure 1B). This finding was further validated in USP11 silenced cells, where ERα activity was significantly abrogated (Figure 1E-J).

Furthermore, USP11 expression was regulated by E2 in ERα+ cells (Figure 2C), and the examination of sub-cellular fractions indicated that this upregulation is occurring in the cell nucleus (Figure 2D). As E2 treatment has no effect on USP11 levels in ERα-negative MDA-MB-231 cells (Figure 2C), we hypothesise that E2 mediates its effect on USP11 via ERα. The exact mechanism of interaction however, warrants further investigation. *In silico* ChIP analysis of ERα binding following E2 stimulation in a series of ER+ breast cancer cell lines failed to demonstrate direct binding to either the USP11 promotor or gene body, suggesting either distal regulation or an indirect mechanism (Supplementary Figure 4).

To further elucidate the relationship between USP11 and ERα, mass spectrometry was used to examine global changes to the proteome and ubiquitinome in breast cancer cells following USP11 suppression. Interestingly, USP11 knockdown resulted in significant changes to the proteome only in the presence of estrogen (Figure 3A-C). This suggests that the role of USP11 in ZR-75-1 breast cancer cells is highly dependent on E2, and perhaps ERα. Further to this, USP11 suppression induced significant changes in the ubiquitinome in the presence of E2, and revealed novel putative substrates of USP11 (Figure 3D-F). Intriguingly, Cyclin D1, a well-described ERα target gene, was ubiquitinated following USP11

suppression and may represent a novel substrate. Cyclin D1 is upregulated in over half of all diagnosed breast cancers, and can regulate ERα in a positive feedback manner. Interestingly, Cyclin D1 expression is also positively correlated with USP11 expression in TCGA breast cancer patients. This observation may be of interest in the link between USP11 and ERα and should be further explored.

USP11 was upregulated in LCC1 and LCC9 breast cancer cells, when compared to their parental MCF-7 cells (Figure 4A). LCC1 cells, derived from MCF-7 breast cancer cells (33), are estrogen independent but are responsive to anti-endocrine agents, suggesting that ERα continues to drive cellular growth but in a ligand-independent manner. LCC9 cells, following exposure to increasing concentrations of fulvestrant (34), are anti-endocrine resistant and depend on other mechanisms for growth and survival. Following knockdown of USP11, ERα transcriptional function was abrogated in LCC1 cells only (Figure 4C). RNA-seq revealed a further role for USP11 in LCC1 cells, with many cell-cycle and ERα target genes suppressed with USP11 knockdown (Figure 4H-I). USP11 suppression had little effect on LCC9 cells (Figure 4D), which are anti-endocrine therapy resistant and rely on alternative growth mechanisms. This strongly supports a role for USP11 in ERα function and suggests that USP11 silencing can interfere with ERα-dependent growth mechanisms. From the perspective of future therapeutic targeting of USP11, our results suggest that patients whose tumors remain driven by ERα would be the most appropriate candidates, for example, those with activating mutations in ERα in recurrent tumors, rendering them less responsive to tamoxifen, but susceptible to abrogation of ERα transcriptional activity.

Finally, high expression of USP11 was significantly associated with poor survival in patients with ERα-positive, but not ERα-negative, tumours (Figure 5A-B), further supporting a role for USP11 in this subtype of breast cancer. Analysis of a USP11-stained TMA further supported this finding at the protein expression level (Figure 5E-H). Many previous studies have outlined the role of DUBs in cancer prognosis, for example, USP22 has been associated with poor prognosis in breast, colorectal and liver cancer, while OTUB1 expression has been associated with a poor outcome in colorectal and ovarian cancer (43). With further studies to support these findings, USP11 may represent a novel marker to be utilised in the clinic to predict patient outcome and response to therapeutic intervention.

With the success of proteasome inhibition in the clinic (44,45) the Ub-proteasome system is becoming an attractive area of therapeutic intervention, and as DUBs are often differentially expressed or activated in tumours, much of the focus around the Ub system has shifted in this direction (46). As most DUBs are cysteine proteases (47), a well-researched class of pharmacological targets, it is feasible to construct specific inhibitors of these enzymes. There are a number of pre-clinical DUB inhibitors in development, for example WP1130, a non-specific inhibitor of USP9x, USP5 and USP14 which induces apoptosis and enhances response to chemotherapy (48) and FT671, a newly developed, specific inhibitor of USP7 which results in stabilisation of p53 and induction of apoptosis (49). As we further interpret the role of DUBs in both physiological and oncogenic pathways, the coming years may see rise some exciting advances in DUB drug discovery (50).

This research demonstrates for the first time, a key role for USP11 in ERα activity in breast cancer. With almost half of patients not responding to current anti-endocrine intervention therapies, it is vital to explore and elucidate novel mechanisms which control ERα function. USP11 may represent a promising route of therapeutic intervention and with further research, may be considered in the DUB drug discovery pipeline for the treatment of ERα-positive breast cancer.

Acknowledgments

This research was predominantly funded by BREAST-PREDICT, the Irish Cancer Society's Collaborative Cancer Research Centre (CCRC13GAL). Additional support was received from the European Union Seventh Framework Programme under the RATHER project 258967, Science Foundation Ireland Career Development Award to D.O'C (15/CDA/3438) and Investigator Programme award OPTi-PREDICT to W.G (15/IA/3104) and the SFI Strategic Partnership "Precision Oncology Ireland" (18/SPP/3522). This work was further supported by a grant from the Dutch Cancer Society through the Oncode Institute to R.B. A.O.C was funded by the Irish Research Council to support this research. D.O'C received additional support from the Human Frontiers Science Programme, UICC and the European Association for Cancer Research.

References

1. Clarke R, Tyson JJ, Dixon JM. Endocrine resistance in breast cancer--An overview and update. Molecular and cellular endocrinology **2015**;418 Pt 3:220-34 doi 10.1016/j.mce.2015.09.035.
2. Dwane L, Gallagher WM, Ni Chonghaile T, O'Connor DP. The Emerging Role of Non-traditional Ubiquitination in Oncogenic Pathways. J Biol Chem **2017**;292(9):3543-51 doi 10.1074/jbc.R116.755694.
3. Haglund K, Di Fiore PP, Dikic I. Distinct monoubiquitin signals in receptor endocytosis. Trends in biochemical sciences **2003**;28(11):598-603 doi 10.1016/j.tibs.2003.09.005.
4. Messick TE, Greenberg RA. The ubiquitin landscape at DNA double-strand breaks. The Journal of cell biology **2009**;187(3):319-26 doi 10.1083/jcb.200908074.
5. Amerik AY, Hochstrasser M. Mechanism and function of deubiquitinating enzymes. Biochimica et biophysica acta **2004**;1695(1-3):189-207 doi 10.1016/j.bbamcr.2004.10.003.
6. Reyes-Turcu FE, Ventii KH, Wilkinson KD. Regulation and cellular roles of ubiquitin-specific deubiquitinating enzymes. Annu Rev Biochem **2009**;78:363-97 doi 10.1146/annurev.biochem.78.082307.091526.
7. Chen ST, Okada M, Nakato R, Izumi K, Bando M, Shirahige K. The Deubiquitinating Enzyme USP7 Regulates Androgen Receptor Activity by Modulating Its Binding to Chromatin. The Journal of biological chemistry **2015**;290(35):21713-23 doi 10.1074/jbc.M114.628255.

8. Dirac AM, Bernards R. The deubiquitinating enzyme USP26 is a regulator of androgen receptor signaling. Molecular cancer research : MCR. Volume 8. United States2010. p 844-54.
9. Stanisic V, Malovannaya A, Qin J, Lonard DM, O'Malley BW. OTU Domain-containing ubiquitin aldehyde-binding protein 1 (OTUB1) deubiquitinates estrogen receptor (ER) alpha and affects ERalpha transcriptional activity. The Journal of biological chemistry. Volume 284. United States2009. p 16135-45.
10. Oosterkamp HM, Hijmans EM, Brummelkamp TR, Canisius S, Wessels LF, Zwart W*, et al.* USP9X downregulation renders breast cancer cells resistant to tamoxifen. Cancer research **2014**;74(14):3810-20 doi 10.1158/0008-5472.can-13-1960.
11. Schoenfeld AR, Apgar S, Dolios G, Wang R, Aaronson SA. BRCA2 is ubiquitinated in vivo and interacts with USP11, a deubiquitinating enzyme that exhibits prosurvival function in the cellular response to DNA damage. Molecular and cellular biology. Volume 24. United States: 2004 American Society for Microbiology; 2004. p 7444-55.
12. Zhou Z, Luo A, Shrivastava I, He M, Huang Y, Bahar I*, et al.* Regulation of XIAP Turnover Reveals a Role for USP11 in Promotion of Tumorigenesis. EBioMedicine **2017**;15:48-61 doi 10.1016/j.ebiom.2016.12.014.
13. Lee EW, Seong D, Seo J, Jeong M, Lee HK, Song J. USP11-dependent selective cIAP2 deubiquitylation and stabilization determine sensitivity to Smac mimetics. Cell death and differentiation **2015**;22(9):1463-76 doi 10.1038/cdd.2014.234.
14. Wiltshire TD, Lovejoy CA, Wang T, Xia F, O'Connor MJ, Cortez D. Sensitivity to poly(ADP-ribose) polymerase (PARP) inhibition identifies ubiquitin-specific peptidase 11 (USP11) as a regulator of DNA double-strand break repair. The Journal of biological chemistry. Volume 285. United States2010. p 14565-71.
15. Orthwein A, Noordermeer SM, Wilson MD, Landry S, Enchev RI, Sherker A*, et al.* A mechanism for the suppression of homologous recombination in G1 cells. Nature **2015**;528(7582):422-6 doi 10.1038/nature16142.
16. Brummelkamp TR, Nijman SM, Dirac AM, Bernards R. Loss of the cylindromatosis tumour suppressor inhibits apoptosis by activating NF-kappaB. Nature **2003**;424(6950):797-801 doi 10.1038/nature01811.

17. Schindelin J, Arganda-Carreras I, Frise E, Kaynig V, Longair M, Pietzsch T*, et al.* Fiji: an open-source platform for biological-image analysis. Nature methods **2012**;9(7):676-82 doi 10.1038/nmeth.2019.
18. Dobin A, Davis CA, Schlesinger F, Drenkow J, Zaleski C, Jha S*, et al.* STAR: ultrafast universal RNA-seq aligner. Bioinformatics (Oxford, England) **2013**;29(1):15-21 doi 10.1093/bioinformatics/bts635.
19. Liao Y, Smyth GK, Shi W. featureCounts: an efficient general purpose program for assigning sequence reads to genomic features. Bioinformatics (Oxford, England) **2014**;30(7):923-30 doi 10.1093/bioinformatics/btt656.
20. Love MI, Huber W, Anders S. Moderated estimation of fold change and dispersion for RNA-seq data with DESeq2. Genome biology **2014**;15(12):550 doi 10.1186/s13059-014-0550-8.
21. McCarthy DJ, Chen Y, Smyth GK. Differential expression analysis of multifactor RNA-Seq experiments with respect to biological variation. Nucleic acids research **2012**;40(10):4288-97 doi 10.1093/nar/gks042.
22. Huang da W, Sherman BT, Lempicki RA. Systematic and integrative analysis of large gene lists using DAVID bioinformatics resources. Nature protocols **2009**;4(1):44-57 doi 10.1038/nprot.2008.211.
23. Subramanian A, Tamayo P, Mootha VK, Mukherjee S, Ebert BL, Gillette MA*, et al.* Gene set enrichment analysis: a knowledge-based approach for interpreting genome-wide expression profiles. Proceedings of the National Academy of Sciences of the United States of America **2005**;102(43):15545-50 doi 10.1073/pnas.0506580102.
24. Unsworth AJ, Bombik I, Pinto-Fernandez A, McGouran JF, Konietzny R, Zahedi RP*, et al.* Human Platelet Protein Ubiquitylation and Changes following GPVI Activation. Thromb Haemost **2019**;119(1):104-16 doi 10.1055/s-0038-1676344.
25. Tyanova S, Temu T, Cox J. The MaxQuant computational platform for mass spectrometry-based shotgun proteomics. Nature protocols **2016**;11(12):2301-19 doi 10.1038/nprot.2016.136.
26. Tyanova S, Temu T, Sinitcyn P, Carlson A, Hein MY, Geiger T*, et al.* The Perseus computational platform for comprehensive analysis of (prote)omics data. Nature methods **2016**;13(9):731-40 doi 10.1038/nmeth.3901.

27. DeNardo DG, Brennan DJ, Rexhepaj E, Ruffell B, Shiao SL, Madden SF*, et al.* Leukocyte complexity predicts breast cancer survival and functionally regulates response to chemotherapy. Cancer discovery **2011**;1(1):54-67 doi 10.1158/2159-8274.cd-10-0028.
28. Ringner M, Fredlund E, Hakkinen J, Borg A, Staaf J. GOBO: gene expression-based outcome for breast cancer online. PloS one **2011**;6(3):e17911 doi 10.1371/journal.pone.0017911.
29. O'Reilly C, Doroudian M, Mawhinney L, Donnelly SC. Targeting MIF in Cancer: Therapeutic Strategies, Current Developments, and Future Opportunities. Medicinal research reviews **2016**;36(3):440-60 doi 10.1002/med.21385.
30. Powell CA, Nasser MW, Zhao H, Wochna JC, Zhang X, Shapiro C*, et al.* Fatty acid binding protein 5 promotes metastatic potential of triple negative breast cancer cells through enhancing epidermal growth factor receptor stability. Oncotarget **2015**;6(8):6373-85 doi 10.18632/oncotarget.3442.
31. Bakos G, Yu L, Gak IA, Roumeliotis TI, Liakopoulos D, Choudhary JS*, et al.* An E2-ubiquitin thioester-driven approach to identify substrates modified with ubiquitin and ubiquitin-like molecules. Nature communications **2018**;9(1):4776 doi 10.1038/s41467-018-07251-5.
32. Yu M, Liu K, Mao Z, Luo J, Gu W, Zhao W. USP11 Is a Negative Regulator to gammaH2AX Ubiquitylation by RNF8/RNF168. The Journal of biological chemistry **2016**;291(2):959-67 doi 10.1074/jbc.M114.624478.
33. Brunner N, Boulay V, Fojo A, Freter CE, Lippman ME, Clarke R. Acquisition of hormone-independent growth in MCF-7 cells is accompanied by increased expression of estrogen-regulated genes but without detectable DNA amplifications. Cancer research **1993**;53(2):283-90.
34. Brunner N, Boysen B, Jirus S, Skaar TC, Holst-Hansen C, Lippman J*, et al.* MCF7/LCC9: an antiestrogen-resistant MCF-7 variant in which acquired resistance to the steroidal antiestrogen ICI 182,780 confers an early cross-resistance to the nonsteroidal antiestrogen tamoxifen. Cancer research **1997**;57(16):3486-93.
35. Ashburner M, Ball CA, Blake JA, Botstein D, Butler H, Cherry JM*, et al.* Gene ontology: tool for the unification of biology. The Gene Ontology Consortium. Nature genetics **2000**;25(1):25-9 doi 10.1038/75556.

939 36. Sun W, Tan X, Shi Y, Xu G, Mao R, Gu X*, et al.* USP11 negatively regulates
940 TNFalpha-induced NF-kappaB activation by targeting on IkappaBalpha.
941 Cellular signalling. Volume 22. England2010. p 386-94.
942 37. Obad S, Olofsson T, Mechti N, Gullberg U, Drott K. Regulation of the
943 interferon-inducible p53 target gene TRIM22 (Staf50) in human T lymphocyte
944 activation. J Interferon Cytokine Res **2007**;27(10):857-64 doi
945 10.1089/jir.2006.0180.
946 38. Dutertre M, Gratadou L, Dardenne E, Germann S, Samaan S, Lidereau R*, et*
947 *al.* Estrogen regulation and physiopathologic significance of alternative
948 promoters in breast cancer. Cancer research **2010**;70(9):3760-70 doi
949 10.1158/0008-5472.can-09-3988.
950 39. Brennan DJ, Rexhepaj E, O'Brien SL, McSherry E, O'Connor DP, Fagan A*, et*
951 *al.* Altered cytoplasmic-to-nuclear ratio of survivin is a prognostic indicator in
952 breast cancer. Clinical cancer research : an official journal of the American
953 Association for Cancer Research **2008**;14(9):2681-9 doi 10.1158/1078-
954 0432.ccr-07-1760.
955 40. Bray F, Ferlay J, Soerjomataram I, Siegel RL, Torre LA, Jemal A. Global
956 cancer statistics 2018: GLOBOCAN estimates of incidence and mortality
957 worldwide for 36 cancers in 185 countries. CA Cancer J Clin **2018**;68(6):394-
958 424 doi 10.3322/caac.21492.
959 41. Xia X, Liao Y, Huang C, Liu Y, He J, Shao Z*, et al.* Deubiquitination and
960 stabilization of estrogen receptor alpha by ubiquitin-specific protease 7
961 promotes breast tumorigenesis. Cancer letters **2019**;465:118-28 doi
962 10.1016/j.canlet.2019.09.003.
963 42. D'Arcy P, Wang X, Linder S. Deubiquitinase inhibition as a cancer therapeutic
964 strategy. Pharmacology & therapeutics **2015**;147:32-54 doi
965 10.1016/j.pharmthera.2014.11.002.
966 43. Pinto-Fernandez A, Kessler BM. DUBbing Cancer: Deubiquitylating Enzymes
967 Involved in Epigenetics, DNA Damage and the Cell Cycle As Therapeutic
968 Targets. Front Genet **2016**;7:133 doi 10.3389/fgene.2016.00133.
969 44. Bold R. "Development of the proteasome inhibitor Velcade (Bortezomib)" by
970 Julian Adams, Ph.D., and Michael Kauffman, M.D., Ph.D. Cancer
971 investigation **2004**;22(2):328-9.

45. Fostier K, De Becker A, Schots R. Carfilzomib: a novel treatment in relapsed and refractory multiple myeloma. OncoTargets and therapy **2012**;5:237-44 doi 10.2147/ott.s28911.
46. Pal A, Young MA, Donato NJ. Emerging potential of therapeutic targeting of ubiquitin-specific proteases in the treatment of cancer. Cancer research **2014**;74(18):4955-66 doi 10.1158/0008-5472.can-14-1211.
47. Shi D, Grossman SR. Ubiquitin becomes ubiquitous in cancer: emerging roles of ubiquitin ligases and deubiquitinases in tumorigenesis and as therapeutic targets. Cancer biology & therapy. Volume 10. United States2010. p 737-47.
48. Chauhan D, Tian Z, Nicholson B, Kumar KG, Zhou B, Carrasco R*, et al.* A small molecule inhibitor of ubiquitin-specific protease-7 induces apoptosis in multiple myeloma cells and overcomes bortezomib resistance. Cancer cell **2012**;22(3):345-58 doi 10.1016/j.ccr.2012.08.007.
49. Turnbull AP, Ioannidis S, Krajewski WW, Pinto-Fernandez A, Heride C, Martin ACL*, et al.* Molecular basis of USP7 inhibition by selective small-molecule inhibitors. Nature **2017**;550(7677):481-6 doi 10.1038/nature24451.
50. Harrigan JA, Jacq X, Martin NM, Jackson SP. Deubiquitylating enzymes and drug discovery: emerging opportunities. Nature reviews Drug discovery **2018**;17(1):57-78 doi 10.1038/nrd.2017.152.

Figure Legends

Figure 1: USP11 silencing abrogates ERα transcriptional activity. **(A)** Functional genomic screening approach, employing a dual luciferase reporter system. **(B)** ERE-luciferase reporter assay depicting the effects of knockdown of 108 DUBs on the transcriptional activity of ERα. ZR-75-1 cells were co-transfected with pools of four non-overlapping shRNAs targeted to each DUB, as well as ERE-luciferase and CMV-renilla reporters. Cells were hormone starved for 48 hours before stimulation with 1 nM E2 for a further 24 hours. Cells were harvested and luciferase activity was detected. **(C)** Triplicate ERE-luciferase reporter assay demonstrating the effect of DUB knockdown on the transcriptional activity of ERα in the presence or absence of E2 stimulation. USP6, a DUB that when knocked down has no effect on ERE-luciferase activity, was used as a baseline measure for statistical testing. **(D)**

Representative Western blot images of HEK293T wild-type (WT) and USP11 knockout cells (KO) transiently transfected with ERα to study receptor function. β-actin was used as a loading control. **(E)** Dual luciferase reporter (DLR) assay examining the effect of USP11 knockout on ERα transcriptional activity. **(F, G)** ERα target gene expression in WT and KO HEK293T cells transfected with ERα or empty vector (EV) and stimulated with E2 for 24 hours. **(H)** USP11 mRNA expression in ZR-75-1 USP11 knockdown and control cells, as determined using qRT-PCR. USP11 was knocked down using two individual siRNAs in ZR-75-1 cells. Knockdown was assessed 72 hours post-transfection. **(I, J)** mRNA expression of ERα target genes in ZR-75-1 USP11 knockdown and control cells, examined 72 hours post-transfection. All experiments were performed in biological triplicate with error bars representing SEM; ** $p<0.01$; *** $p<0.001$; **** $p<0.0001$, student's t-test.

Figure 2: Upregulation of USP11 in breast cancer cells following E2 stimulation. (A) Western blot displaying USP11 and ERα protein expression across a panel of ERα+ cell lines. β-actin was used as a loading control. **(B)** Correlation plot based on densitometric analysis of USP11 and ERα Western blot in Figure 2A. Values are expressed as a percentage of the total area of all bands. **(C)** USP11 and ERα expression in ZR-75-1, MCF7 and MDA-MD-231 cells following treatment with either E2 alone or E2 and 4-hydroxytamoxifen (4HT) combined over varying time points. EtOH alone or ETOH/DMSO at a concentration of 1:1000 each were used as vehicle controls. β-actin was used as a loading control. **(D)** Subcellular protein fractions depicting USP11 expression following E2 treatments over varying time points. Tubulin, trimethyl histone H3 and cytochrome-C were used as cytoplasmic (C), nuclear (N) and membrane (M) controls, respectively. **(E)** Immunofluorescent images of USP11 nuclear expression in ZR-75-1 cells in the presence and absence of E2. Scale bars are equal to 10 μM. Experiments were performed in biological triplicate.

Figure 3: USP11 silencing significantly alters the protein and ubiquitin landscape in ZR-75-1 cells treated with E2. (A) Western blot of matched protein utilised for mass spectrometry. Two USP11 knockdown cell lines were used (shUSP11_1 and shUSP11_4) and a non-targeting control (NTC), in the presence

and absence of 1 nM E2. **(B)** Heatmap representing the intensity of each detected protein (3572 in total) in each sample and technical replicate. Coloured squares represent Z-score intensity values, where the colour range (red, black green) represents the intensity range (high, moderate, low, respectively). **(C - F)** Volcano plots representing the fold change (y-axis) and significance (y-axis) of differentially expressed proteins in USP11 knockdown and control (NTC) cells. Red dots represent proteins significantly upregulated in USP11 knockdown cells when compared to control; blue dots represent proteins significantly upregulated in NTC cells when compared to knockdown. Samples were analysed in **(C, D)** the presence and **(E, F)** absence of E2. **(G)** Heatmap representing the intensity of each detected ubiquitinated protein (1539 in total) in each sample and technical replicate. **(H & I)** Volcano plots representing differentially ubiquitinated proteins in USP11 knockdown and control (NTC) cells. Red dots represent proteins significantly ubiquitinated in USP11 knockdown cells when compared to control; blue dots represent proteins significantly ubiquitinated in NTC cells when compared to knockdown. Samples were again analysed in **(H)** the presence and **(I)** absence of E2. Statistical analysis was performed using a two-sided t-test (unpaired); FDR was set to 5% (0.05).

Figure 4: USP11 expression is upregulated in LCC1 and LCC9 cells and silencing affects ERα transcriptional activity in LCC1 cells only. (A, B) USP11 and ERα protein and mRNA expression in MCF7, LCC1 and LCC9 cells, as determined by **(A)** Western blotting and **(B)** qRT-PCR, respectively. β-actin was used as a loading control. **(C)** siRNA-mediated knockdown of USP11 in LCC1 cells, followed by ERα target gene mRNA expression. **(D)** siRNA-mediated knockdown of USP11 in LCC9 cells, followed by ERα target gene mRNA expression. Gene expression is normalised to 18S gene expression in all qRT-PCR results. **(E)** Venn diagrams illustrating the number of DE genes with USP11 knockdown, identified by RNA-seq. Two independent siRNAs targeted to USP11 were used and DE genes common to both were subject to further analysis. **(F)** Venn diagram highlighting the total number of DE genes in each cell line as well as the overlapping DE genes between both cell lines. **(G)** Bar graphs depicting the number of significantly down- (blue) and upregulated (red) genes in LCC1 and LCC9 USP11 knockdown cells. **(H)** Bar graph portraying the 10 most significant GO pathways associated with downregulated genes in LCC1 USP11 knockdown cells. **** p< 0.0001, Benjamini

adjusted (FDR). **(I)** Enrichment plot depicting the enrichment of cell cycle pathway genes in LCC1 USP11 knockdown and control cells. **(J)** RNA-seq validation in LCC1 USP11 knockdown cells by qRT-PCR. Downregulation of the ERα target genes *TOP2A*, *BLM* and *BRCA1* was confirmed in LCC1 USP11 knockdown cells. Upregulation of the tumour suppressor TRIM22 was also confirmed. Gene expression is normalised to 18S gene expression. **(K)** Pie chart highlighting the number of downregulated genes in LCC1 USP11 knockdown cells which overlap with the Dutertre dataset. All experiments were performed in biological triplicate with error bars representing SEM; * $p<0.05$; ** $p<0.01$; *** $p<0.001$; student's t-test.

Figure 5: USP11 represents a poor prognostic marker in ERα+ breast cancer. **(A-D)** *In silico* survival analysis using pooled microarray patient data from the Gene Expression Based Outcome for Breast Cancer Online (GOBO) tool (28). **(A, B)** Kaplan-Meier curves correlating high (red) and low (grey) USP11 expression with overall survival (OS) in both **(A)** ERα-positive and **(B)** ERα-negative cohorts. **(C, D)** Multivariate analysis of USP11 expression in **(C)** ERα-positive and **(D)** ERα-negative cohorts. USP11 expression was compared against multiple clinical parameters and a hazard ratio was determined for each parameter. **(E)** USP11 immunohistochemical staining of a 144 breast cancer patient tissue microarray; 103 ERα-positive patients were available for final analysis. **(F-H)** Kaplan-Meier survival analysis correlating USP11 expression with **(F)** overall survival (OS), **(G)** breast cancer-specific survival (BCSS) and **(H)** recurrence free survival (RFS). A p-value < 0.05 was considered statistically significant.

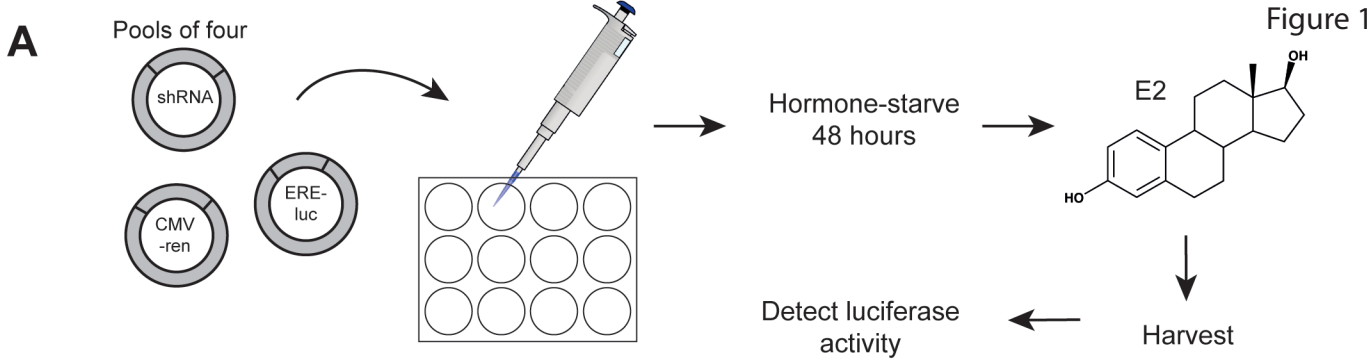

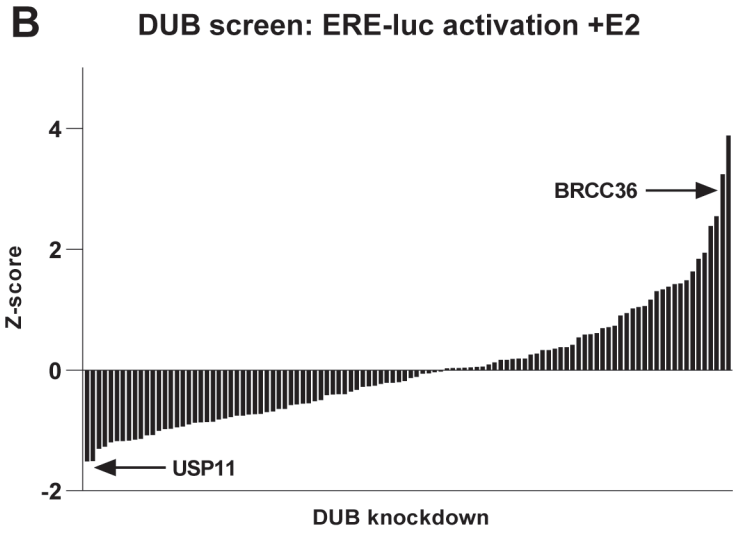

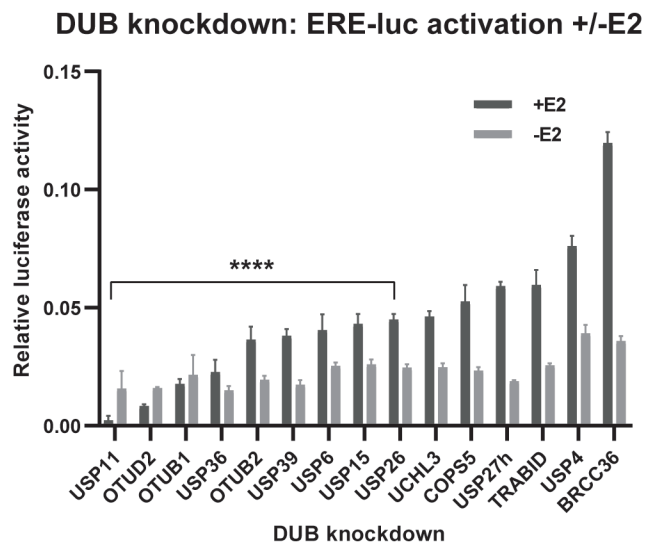

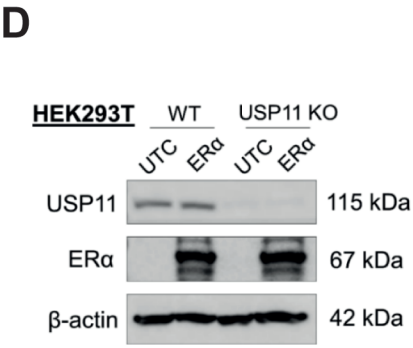

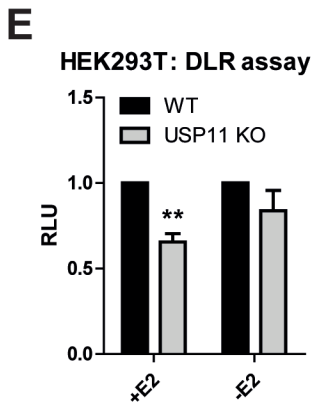

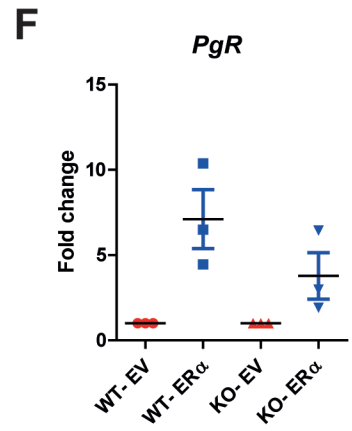

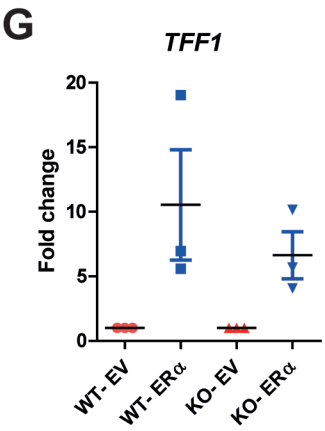

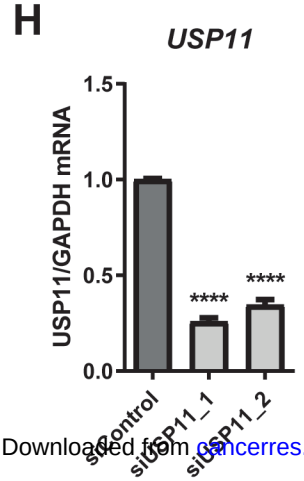

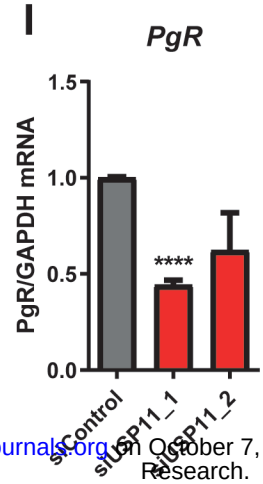

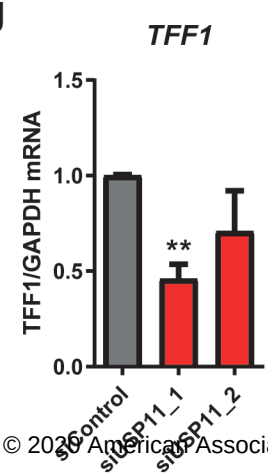

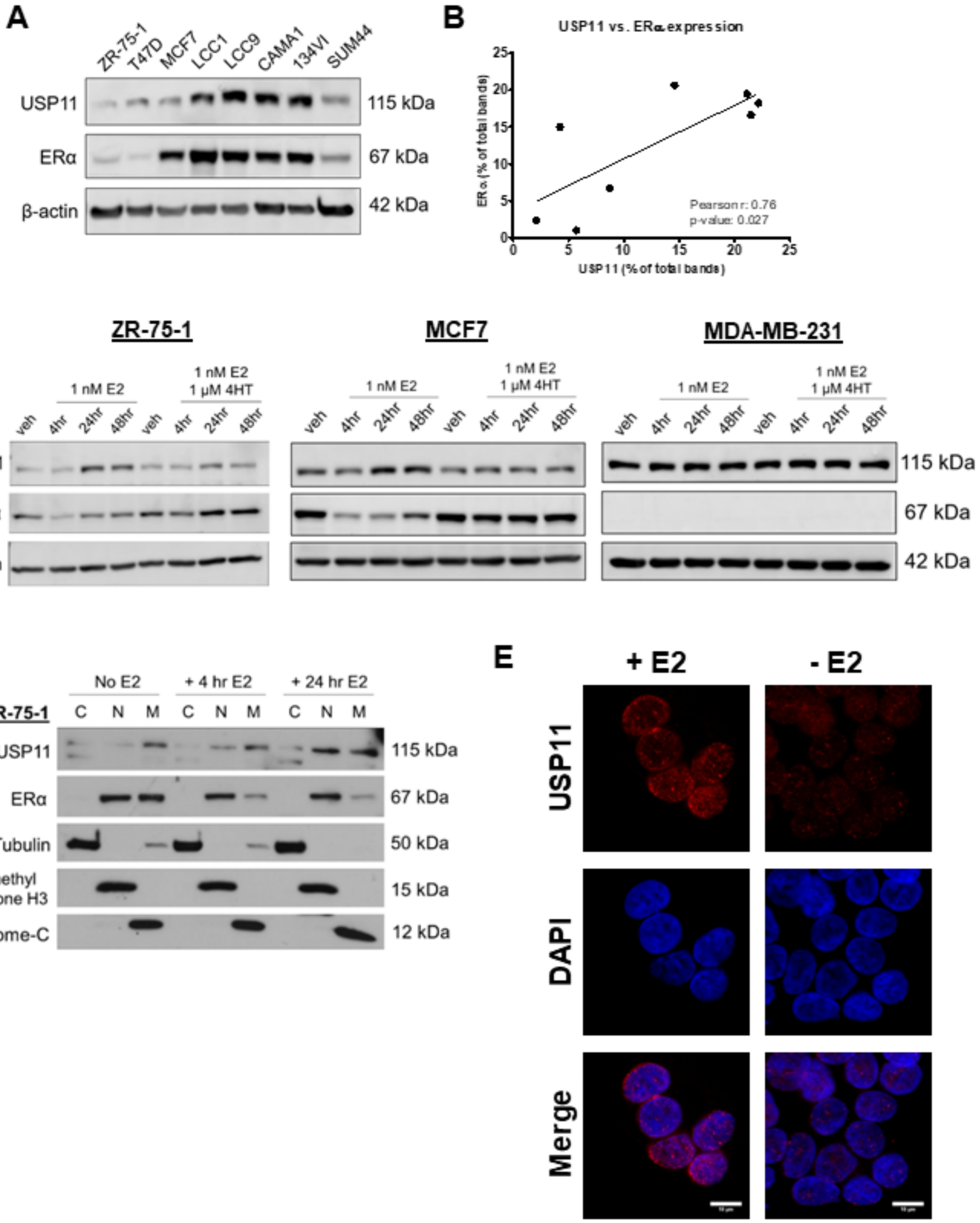

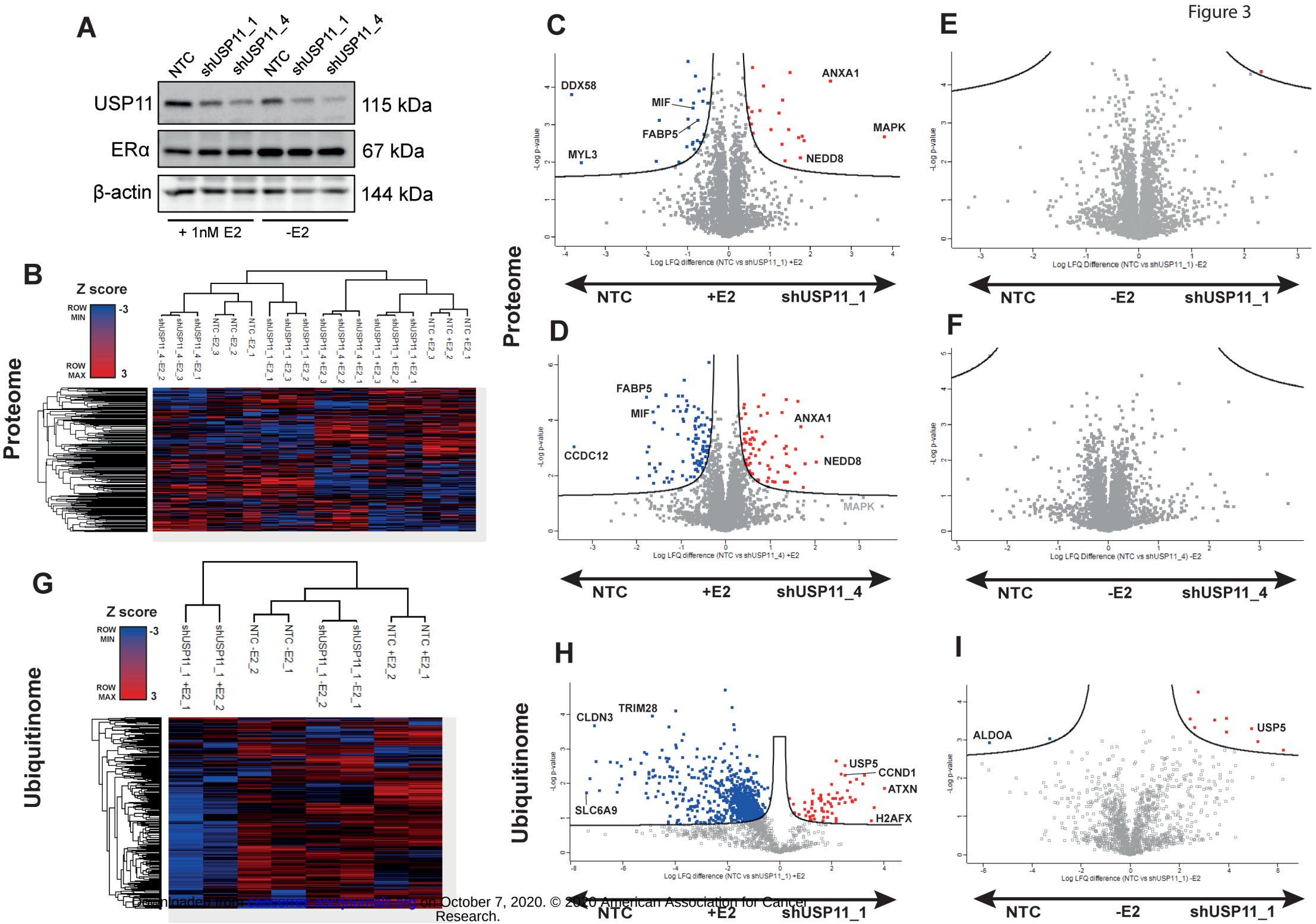

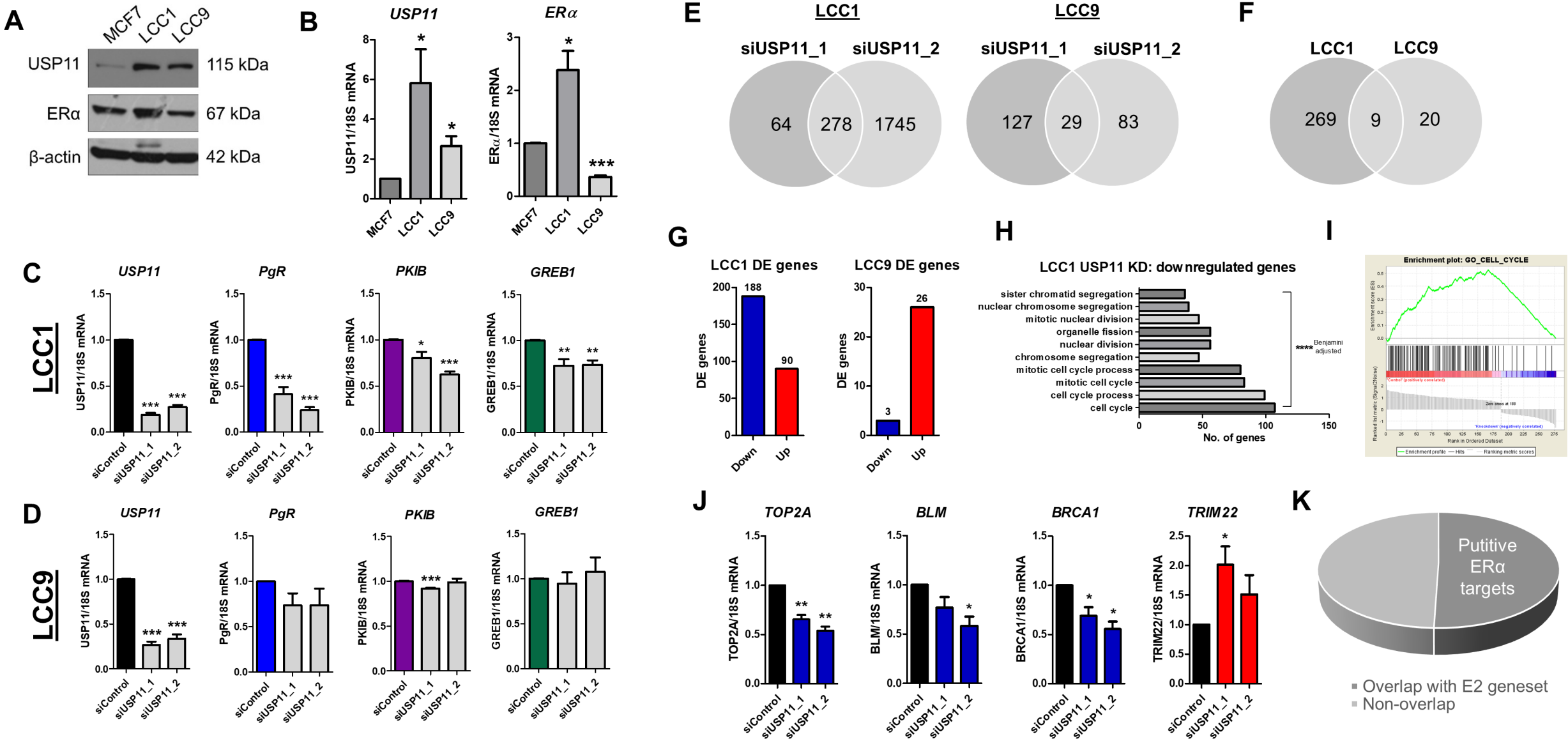

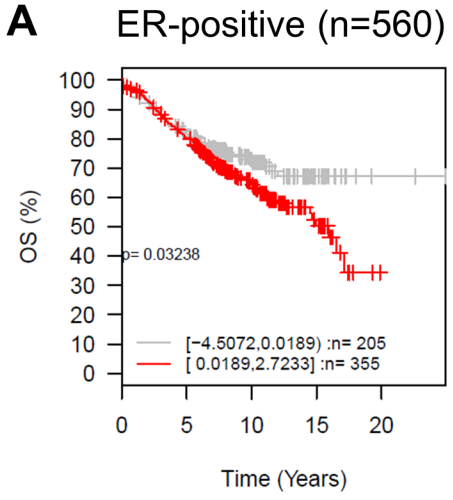

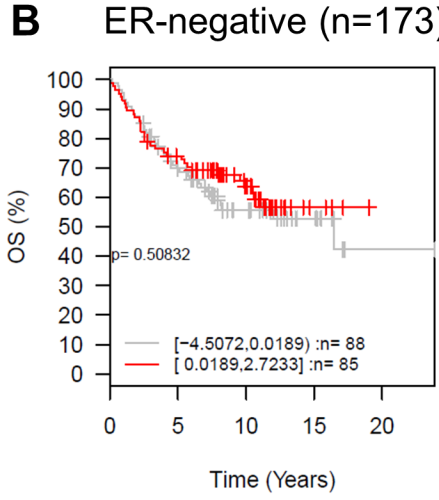

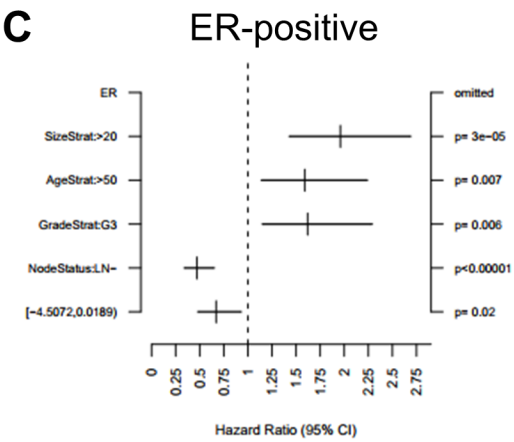

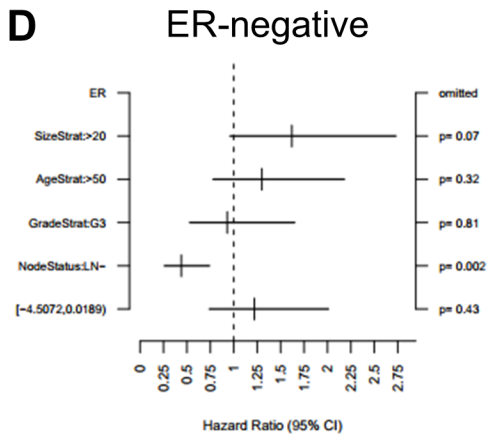

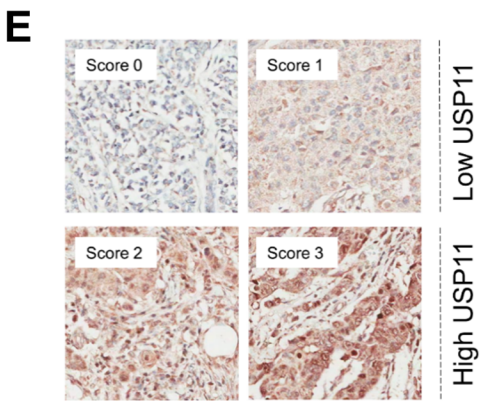

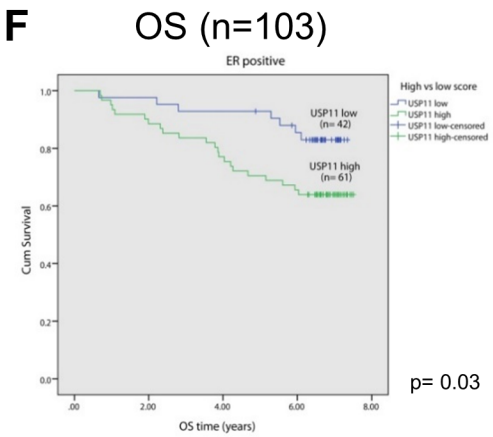

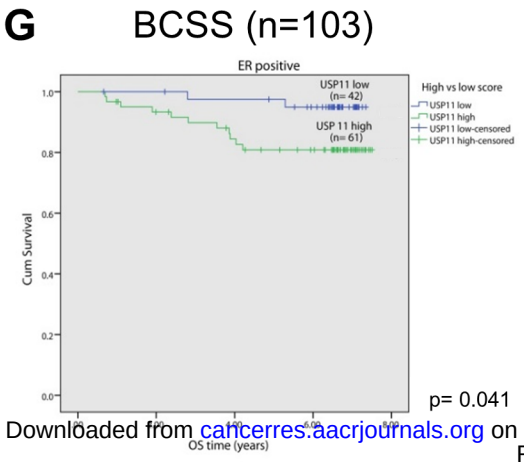

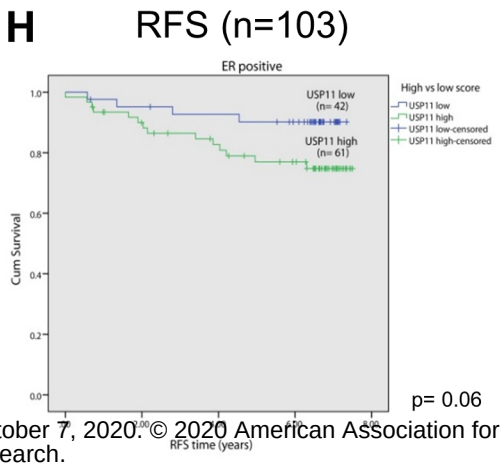

AACR American Association for Cancer Research

Cancer Research

The Journal of Cancer Research (1916–1930) | The American Journal of Cancer (1931–1940)

A functional genomic screen identifies the deubiquitinase USP11 as a novel transcriptional regulator of ER α in breast cancer

Lisa Dwane, Aisling E. O'Connor, Sudipto Das, et al.

Cancer Res Published OnlineFirst October 1, 2020.